Shear Modulus of Sand Subjected to Simple Shear

Supot TEACHAVORASINSKUN[1], Satoru SHIBUYA[2]
and
Fumio TATSUOKA[3]

SYNOPSIS

A laboratory investigation has been carried out into stiffness of a quartz sand, Toyoura sand, for a wide range of strains from 10^{-6} to the peak. Hollow cylindrical specimens were anisotropically consolidated and subjected to drained simple shear in a fully automated torsion shear apparatus. Shearing took place in two fashions;i.e. the shear stress on the horizontal plane was monotonically increased to failure(static loadings), and it was applied in a cyclic manner with the amplitude being increased in steps(dynamic loadings). With an aid of the small strain measurements, the genuine linear elastic region for each type of tests has been identified for the limiting shear strain of 5×10^{-6} below which the two types of loadings give rise to virtually the same stiffness. Furthermore, the conventional hyperbolic fitting has been found appropriate to represent the stress-strain relationship for the case of cyclic loadings, however this fitting underestimated the strain-level dependency of the stiffness of the specimens which subjected to monotonic loadings.

---

1) Graduate student, Institute of Industrial Science, University of Tokyo.
2) Research Assistant, ditto.
3) Associate Professor, ditto.

1. INTRODUCTION

Figure 1 shows a simulation of the simple shear mode of deformation in a hollow cylindrical specimen having a three-dimensional axes. It involves zero horizontal extension in the direction of shear (i.e. t-direction) together with the plane strain in the orthogonal r-direction. The shear strain γ_{rt} develops when the corresponding shear stress is applied.

In geotechnical engineering practice, the simple shear mode of deformation is often encountered for soil elements, for instance, in a horizontal ground subjected to seismic loadings, adjacent to displacement piles, along the horizontal part of the failure surface beneath an embankment and so on. In these cases, the pre-peak stress-strain behaviour must be evaluated beforehand, as well as the strength, when analysing deformation of the ground or predicting the load-displacement relationship for the case of displacement piles. In doing so, two types of loadings, i.e. monotonic(=static) loadings and cyclic(=dynamic) loadings, should be distinguished according to the in-situ loading conditions.

The stiffness of isotropically consolidated sands as subjected to cyclic loadings has been intensively investigated in the laboratory using a resonant-column apparatus or a torsion shear apparatus (e.g., Hardin and Drnevich, 1972; Iwasaki, Tatsuoka and Takagi, 1978 among others). In these devices the soil specimens were sheared under quasi simple shear conditions. In general, the strain levels which may be investigated in a resonant-column apparatus range from 10^{-6} to 10^{-4}, whereas those investigated in a conventional torsional shear apparatus are usually larger than 10^{-4}.

Despite that the dynamic properties of sands have been a major interest in soil dynamics, an understanding of the soil stiffness subjected to monotonic loadings is at present relatively poor, especially for the scope of small strains, say, shear strains less than 10^{-4}. This is due to the poor measurements of displacements of the soil specimens in the laboratory. In the last decade, a few attempts have been made to measure the

stiffness of soils, especially for stiff soils, in the small strain region when subjected to monotonic loadings (Burland and Symes, 1982; Jardine et al.,1984; Tatsuoka,1986; Shibuya and Hight,1987; Goto,1987; Clayton,1989; Shibuya, Tatsuoka and Kong,1990). However, yet a better understanding of the effects of the loading conditions on the stiffness is highly desirable so as to properly assess the stiffness of in-situ soils which may be subjected to complicated loading paths.

This paper presents the results of monotonic and cyclic torsion shear tests performed on Toyoura sand. In these tests, the shear strains were measured with an accuracy of the order of 10^{-6}. The objective of the tests was thus to observe the missing link of the secant stiffness between the monotonic and cyclic loading tests. Accordingly, the interpretation of the test results highlights the effect of the pattern of loadings on the dependency of the shear modulus in relation to the shear strain levels.

2. APPARATUS USED

The Institute of Industrial Science torsion shear apparatus (TSA) was used for the study. The apparatus and computer-based servo-control system have been described in details by Pradhan et al. (1988).

To simulate the simple shear mode of deformation in TSA, a hollow cylindrical specimen with dimensions of 6cm i.d.,10cm o.d. and 20cm high was sheared under drained conditions in a manner that the shear strain γ_{at} was imposed at a constant rate of 0.01% per minute. During shearing both the inner and outer cell pressures were adjusted to maintain no lateral movements of the specimen walls. Furthermore the axial stress was also maintained at a constant value throughout shear. The general concept of the computer based servo-control system is shown in Fig.2. Based on information on the current state of the specimen, the axial load and cell pressures were controlled so as to satisfy the simple shear conditions by using three Electric/Pneumatic(E/P)

transducers, each capable of changing a pressure as small as 0.005 kgf/cm^2. The tolerances adopted for the control were $\pm$0.005 kgf/cm^2 for the axial stress and $\pm$0.002% for ε_r and ε_t, respectively. For the latter a correction is made to take account of the membrane(0.2mm thick) penetration. In all tests presented in this paper, these tolerances were strictly satisfied at least for the pre-peak region (Pradhan et al, 1988).

In the current version of the TSA, a modification has been made for the tangential displacement measurements (Fig.3). In the previous system, the rotation of the top cap was measured by means of a rotational transducer (potensiometer). By using this, the resolution of the measurement was, for the size of specimen used, as good as 7×10^{-5} in terms of γ_{zt}. As can be seen in Fig.3, the newly developed 'Relay' system incorporates two proximity transducers, with the capacities of a 4 mm and a 8 mm, together with the potensiometer. The resolution of the proximity transducers decreases in proportion to the capacity. The 'Relay' measurement is such that, as shear strain increases, the measurement is relayed in sequence of a 4 mm proximeter, a 8 mm proximeter and the potensiometer for the ranges of shear strain(γ_{zt}) corresponding respectively to less than 0.3%, less than about 1%, and more than 1%. The resolution of a proximity transducer with a 4 mm capacity is 0.4 μm in the current system. This enables the shear strain to be measured by an accuracy of 10^{-6}. Therefore, by having the 'Relay' system, it is possible to measure the shear strain for a wide range between 10^{-6} and 10^{-1}.

The average stresses and strains used for the tests are those described by Hight, Gens and Symes (1983).

3. DESCRIPTION OF TESTS PERFORMED

The specimens were prepared by pluviating dry Toyoura sand through air (i.e. air-pluviation method). The density was controlled by having different free fall heights during the preparation. The specimens were first subjected to a suction of 0.05kgf/cm^2, then the initial void ratio $e_{0.05}$ was measured.

The specimens were anisotropically consolidated against a constant back pressure of 2 kgf/cm^2 using a fixed value of $K(=\sigma_r/\sigma_a)$ for each test. The details of consolidation together with some results are summarized in Table 1. It is to be noted that particular values of K equal to 0.36 and 0.41 gives rise to approximately Ko conditions for loose ($e_{0.05}\fallingdotseq 0.8$) and dense ($e_{0.05}\fallingdotseq 0.7$) specimens, respectively(Okochi and Tatsuoka, 1984). The prescribed consolidation paths are sketched in Fig.4.

4. PRESENTATION OF TEST RESULTS

Figures 5 and 6 show the relationship between the shear stress and the shear strain for two groups of tests using loose and dense specimens, respectively. In each group of tests, the difference of the stress-strain response is due to the different consolidation pressures applied. The inset of Fig.7 is the initial part of the stress-strain relationship for the shear strain less than 7×10^{-6} for a dense specimen(Test MTS09). As can be seen in the figure, the linear relationship was observed for shear strain less than about 7×10^{-6} irrespective of the density and the initial stress state of the specimen. The inclination in this portion was thus taken as the maximum shear modulus G_{max}. The values of G_{max} are listed in Table 1.

In the monotonic loading tests, a small unloading-reloading cycle was imposed in the early stage of shear to examine an elastic property of the material at small strain levels. An example is shown in Fig.8, in which the cycle was applied when the shear strain reached to about 3.5×10^{-5}. It was observed that the response was not a purely elastic, however the secant shear modulus corresponding to double amplitude of shear strain of approximately 2×10^{-5} was more or less equal to G_{max} determined from the virgin loading. This was typical of the results obtained.

A variation of mean effective stress $t=(\sigma_1+\sigma_3)/2$ during simple shear is shown in Fig.9. In this figure, the shear strain levels are indicated along the stress path. It is important

that the mean effective stress remains more or less constant up to a shear strain level of approximately 10^{-2}. The strain level corresponds to the shear stress of about 50% of the maximum shear stress, τ_{max}. The mean effective stress increased gradually as shear progressed. The tendency was similar for all tests. This means that the shear modulus beyond the level of shear strain of about 10^{-2} was affected, to a certain extent, by the change in mean effective stress. The discussion of the test results therefore sticks to the region with shear strains less than 10^{-2}.

5. DISCUSSION

The definitions of secant shear moduli for the monotonic loading tests are sketched in Fig.10(a). In this figure, the equivalent shear modulus G_{eq} which stands for the secant shear modulus for the unloading-reloading cycle (see Fig.8) is shown together with the secant shear modulus, G_s.

A comparison of soil stiffness associated with two modes of loadings, i.e. monotonic loadings and cyclic loadings, is made in terms of the secant shear moduli. Figure 10(b) shows the coincidence of the secant shear moduli of the equivalent shear modulus, G_{eq} for cyclic tests and of G_s for monotonic loading tests. This is the case of the Masing's second rule for the material having an isotropic property in the stress-strain response. The symmetry of the stress-strain relationship is initially assured in the case of simple shear since the shear stress is applied on the horizontal plane. As can be seen in Fig.10(b), the value of G_{eq} should be examined in relation to the single amplitude of shear strain γ_{SA} so as to make a fair comparison with the relationship between G_s and γ obtained from the monotonic loading tests.

Figures 11(a) and 11(b) show the relationship of G_s versus γ for a dense specimen (MTS09, p'=1.15 kgf/cm^2) and a loose specimen (MTS28, p'=1.21 kgf/cm^2), respectively. It should be noted that the threshold strain beyond which the value of G_s decreases as the shear strain increases is γ_{at} equal to about

7×10^{-6} irrespective of the density of the specimens. The maximum stiffness, G_{max}, which was determined by regressing the data in the initail linear region is plotted against the initial void ratio and the mean effective stress, $p'=(\sigma_1+\sigma_2+\sigma_3)/3$ (Fig.12). It increased as both density and the mean effective stress increased (see also Table 1).

The effect of the mean effective stress on the stress-strain relationship is examined in Fig.13, in which the normalized stiffness, G_s/G_{max}, is plotted against γ_{at}. For the range of p' examined (p':0.6～1.2 kgf/cm^2), the effect of p' is not remarkable for loose specimens. A similar tendency was also observed for dense specimens. This differs from the results of cyclic tests reported by Iwasaki et al.(1978) in which the strain level dependency of G_{eq}/G_{max} was larger as p' decreased.

A hyperbolic function using only two quantities of the maximum shear stress τ_{max} and G_{max} is often employed to represent the overall stress-strain relationship. The original equation proposed by Kondner(1963) takes the following form:

$$\tau = \frac{\gamma}{(1/G_{max} + \gamma/\tau_{max})} \qquad (1)$$

The solid line in Fig. 7 represents the hyperbolic stress-strain relationship using the measured values of G_{max} and τ_{max}. It is clear that the hyperbolic relationship (eqn(1)) is utterly improper to represent the overall stress-strain relationship. Provided that the stress-strain relationship satisfies eqn(1) throughout shear, the values of both G_{max} and τ_{max} can be estimated without knowing the real G_{max} and τ_{max}. This may be done by having a plot of γ/τ versus γ. The data, which may exclude the very initial and the right peak portions of the stress-strain relationship, can be regressed using a linear function to extrapolate the values of G_{max} and τ_{max}. An example is shown for a dense specimen in test MTS09 (Fig.14). Figures 15(a) and 15(b) show the relations between the estimated values of G_{max} and τ_{max}, which are described as G_{hyper} and τ_{hyper}, and those measured, for two groups of tests using dense and loose specimens,

respectively. The ratio of τ_{hyper}/τ_{max} is, irrespective of the mean effective stress, close to unity in the case of loose specimens and 1.05 for the dense specimens. However, the difference is remarkable for G_{max} in a manner that the value of G_{hyper}/G_{max} increased gradually with the increasing p', but the ratio was at most 0.3 even for the dense specimens. The solid line shown in Fig.14 is a hyperbolic stress-strain relationship calculated using the values of G_{hyper} and τ_{hyper}. This confirms that the hyperbolic function is appropriate only when the specimens were cyclically sheared.

A comparison between G_s and G_{eq} for dense specimens is made in Fig.16, in which the secant shear moduli are plotted against the corresponding shear strains. In this figure, the results of cyclic tests measured in a resonant-column device for γ less than 10^{-4} and in a torsional shear apparatus for γ more than 10^{-4} (Iwasaki et al,1978) are also shown for a comparison (see also Fig.11). For the results obtained from these three different types of tests, the followings are to be noted.

(i) In the region of shear strain less than 7×10^{-6}, the secant shear moduli amongst the monotonic test (MTS09) and the cyclic tests (CTS02 and the resonant-column tests performed by Iwasaki et al.(1978)) practically coincided with each other and these remained more or less constant.

(ii) For the cyclic simple shear test performed in the present study, the secant shear modulus for a fixed shear strain level increased gradually as the number of loadings increased particularly at larger strain amplitudes.

(iii) The aspect of the dependency of G_{eq} on γ_{SA} was similar between the cyclic simple shear test and the resonant column and torsional shear tests performed by Iwasaki et al.

(iv) The reduction of the secant shear modulus with respect to γ was larger in the monotonic loading test than those of the cyclic tests.

The coincidence of G_{eq} and G_s, together with the linearity in the stress strain relationship in the early stage of shearing(see Fig.7) means that the response of the sand is linear-elastic for the shear strain less than about 7×10^{-6}. Furthermore, it should be

pointed out that at a constant mean effective stress p', the effect of initial shear on G_{max} was not significant at all for the initial stress ratio σ_r/σ_a up to 0.36. This matches results of tests reported by Tatsuoka et al.(1979). The second and fourth remarks strongly suggest that the Masing's second rule does not apply to the behaviour of the natural sand.

The shapes of the secant shear modulus versus the shear stress relationship are examined in Fig.17, in which the normalized shear moduli, G_s/G_{max} and G_{eq}/G_{max}, are plotted against the normalized shear stress, τ_{at}/τ_{max}. When a hyperbolic stress-strain relationship shown in eqn(1) is assumed, two parameters should be related as;

$$G_s/G_{max} \text{ or } G_{eq}/G_{max} = 1-\tau_{at}/\tau_{max} \qquad (2)$$

The hyperbolic relationship is drawn using a solid line. It is clear that the relationship between G_{eq} and γ in the cyclic loading tests may well be approximated using a hyperbolic function (Iwasaki et al.,1978), but the hyperbolic relationship overestimates the stiffness for the monotonic loading tests throughout shear.

Another comparison of the stiffness between the torsional simple shear tests and the resonant-column tests (Iwasaki et al.) is made in Fig.18, in which the secant shear moduli are directly compared for different strain levels. For the normally consolidated specimens, the cyclic tests give higher stiffness than the monotonic loading tests, however the difference in stiffness between two types of tests is not significant for the overconsolidated specimens. The effects of the stress history on the stress-strain relationship are discussed in details by Teachavorasinskun et al.(1989).

6. CONCLUSIONS

The stiffness of Toyoura sand when subjected to drained simple shear has been observed for a wide range of shear

strain from 10^{-6} to the peak. The major findings are summarized in the followings.

(1) The linear elastic response was observed for the shear strain less than about $7x10^{-6}$ in which region the stress-strain relationship in the monotonic tests was linear and the secant shear moduli between the monotonic and the cyclic tests were practically identical.

(2) The limiting shear strain which defines the boundary of the linear elastic response appears to be unaffected by the density and by the mean effective stress for the normally consolidated specimens.

(3) The aspect of the dependency of the secant shear modulus on the shear strain was different for the monotonic loading and the cyclic loading. The reduction of stiffness with the increasing shear strain was much larger in the monotonic loading tests than the cyclic tests.

(4) The relationship between secant shear modulus and the shear strain may be approximated using a hyperbolic function for the case when the shear stress was applied in a cyclic manner, however, the hyperbolic stress-strain relation overestimates the true stiffness of the sand in the case of the monotonic loading tests.

REFERENCES

1) Burland,J.B. and Symes,M.J.(1982): "A simple axial displacement gauge for use in the triaxial apparatus," Geotechnique, Vol.32,No.1,pp-62-65.

2) Clayton,C.R.I., Khatrush,S.A., Bica,A.V.D. and Siddique,A. (1989): "The use of hall effect semiconductors in geotechnical instrumentation," Geotechnical Testing Journal, Vol.12, No.1,

pp.69-76.

3) Goto,S. (1987): "Strength and deformation characteristics of granular materials in triaxial tests," Dr. Eng. Thesis, University of Tokyo.

4) Hardin,B.O. and Drnevich,V.P. (1972): "Shear modulus and dumping in soils: measurement and parameter effects," ASCE, Vol.98, No.SM6, pp.603-624.

5) Hight,D.W., Gens,A. and Symes,M.J. (1983): "The devolopment of a new hollow cylinder apparatus for investigating the effects of principal stress rotation in soils," Geotechnique, Vol.33, No.4, pp.355-384.

6) Iwasaki,T., Tatsuoka,F. and Takagi,Y. (1978): "Shear moduli of sands under cyclic torsional shear loading," Soils and Foundations, Vol.18, No.1, pp.39-56.

7) Jardine,R.J., Burland,J.B. and Symes,M.J. (1984): "The measurement of soil stiffness in the triaxial apparatus," Geotechnique, Vol.34, No.3, pp.323-340.

8) Kondner,R.L. (1963): "Hyperbolic stress-strain response: cohesive soil," Journal of ASCE, Vol.89, No.SM1,pp.115-143.

9) Okochi,Y. and Tatsuoka,F. (1984): "Some factors affecting K_o-values of sand measured in triaxial cell," Soils and Foundations, Vol.24, No.3, pp.52-68.

10) Pradhan,T.B.S.,Tatsuoka,F. and Horii,N. (1988): "Simple shear testing on sand in a torsional shear apparatus," Soils and Foundations, Vol.28, No.2, pp.95-112.

11) Shibuya,S. and Hight,D.W. (1987): "A bounding surface of granular materials," Soils and Foundations, Vol.27, No.4, pp.123-136.

12) Shibuya,S.,Tatsuoka,F and Kong,X.J. (1990): Discussion in the Proc. of XII ICSMFE, Rio de Janeiro (to be published).

13) Tatsuoka,F., Iwasaki,T., Fukushima,S. and Sudo,H. (1979): "Stress conditions and stress histories affecting shear modulus and dynamic damping of sand under cyclic loading," Soils and Foundations, Vol.19, No.32, pp.29-43.

14) Tatsuoka,F. (1986): "Some recent developments in triaxial testing systems for cohesionless soils," Advanced Triaxial Testing Systems for Cohesionless Soils, ASTM STP977, pp7-67.

15) Teachavorasinskun,S., Shibuya,S. and Tatsuoka,F. (1989): "Stiffness of sand in simple shear," Proc. of 24th annual meeting of JSSMFE, Tokyo, pp.523-526.

16) Teachavorasinskun,S., Shibuya,S. and Tatsuoka,F. (1990): "Stress history Dependency of stiffness of a sand observed in simple shear," Seisan-Kenkyu, Vol.42, No.3 (to be published).

Table 1. Summary of initial conditions and some results of NC specimen (OCR=1.0)

TEST No.	eo.os	σ_a	K-value[1]	p'[2]	τ_{max}	G_{max}[3]	γ_r (x 10^{-3})[4]
MTS06	0.694	1.00	0.36 ☆	0.58	0.75	930	0.807
MTS07	0.690	1.67	0.36 ☆	0.97	1.22	1240	0.984
MTS09	0.696	2.00	0.36 ☆	1.15	1.42	1305	1.092
MTS26	0.803	1.00	0.41 ☆	0.60	0.65	730	0.890
MTS27	0.791	1.67	0.41 ☆	1.01	1.06	970	1.093
MTS28	0.783	2.00	0.41 ☆	1.21	1.31	1100	1.195
CTS01 ▲	0.788	1.67	0.41 ☆	0.95	1.15	1050	1.001
CTS02 ▲	0.662	1.67	0.36 ☆	0.96	1.26	1250	1.001

1) $K = \sigma_r'/\sigma_a'$

2) $p' = [(\sigma_a' + 2\sigma_r')/3]_{initial}$

3) $G_{max} = [\tau_{at}/\gamma_{at}]$ at $\gamma_{at} < 7 \times 10^{-6}$

4) $\gamma_r = \tau_{max}/G_{max}$

☆ → Ko-consolidation (= 0.52 x eo.os)

▲ → Cyclic test

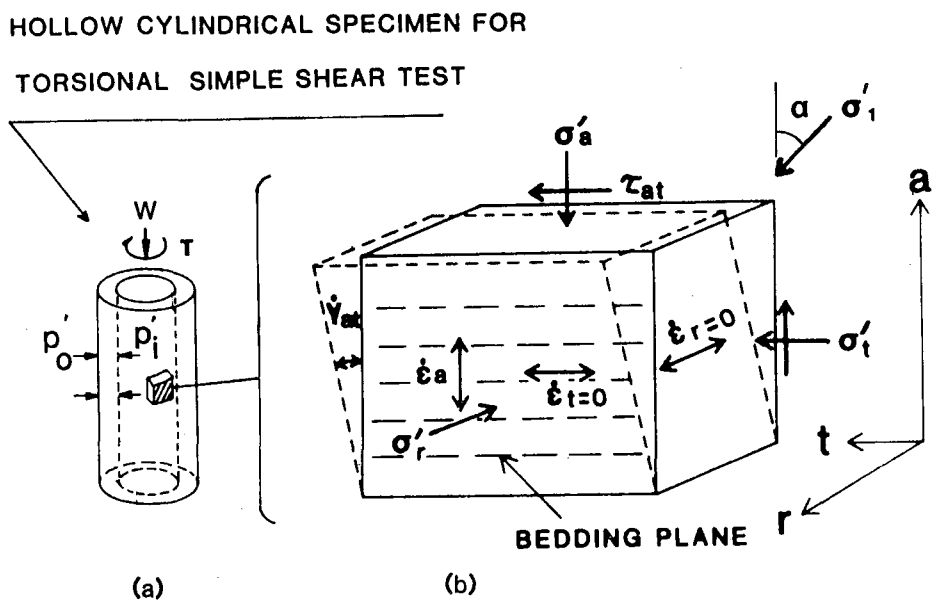

Fig.1 A simulation of simple shear mode of deformation in a hollow cylindrical specimen.

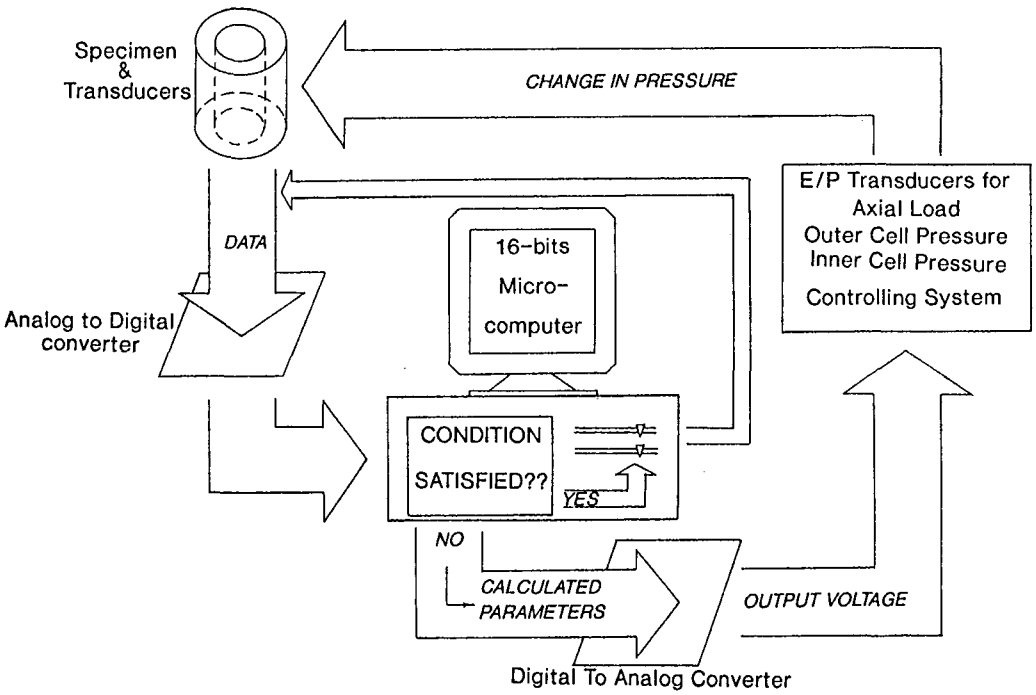

Fig.2 A servo-control used to simulate simple shear

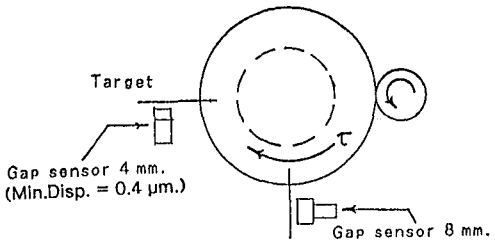

Fig.3 A newly developed 'Relay' system to measure rotational displacement of the hollow cylindrical specimen.

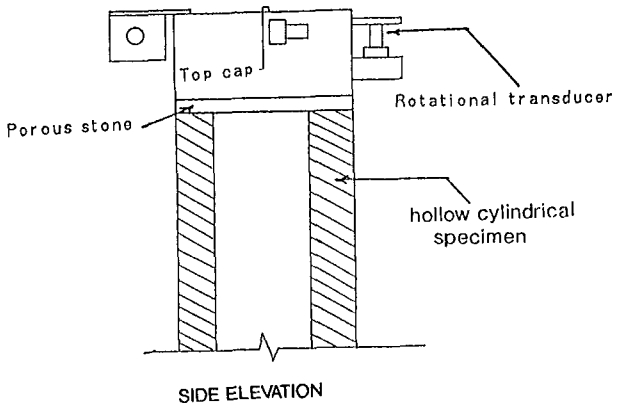

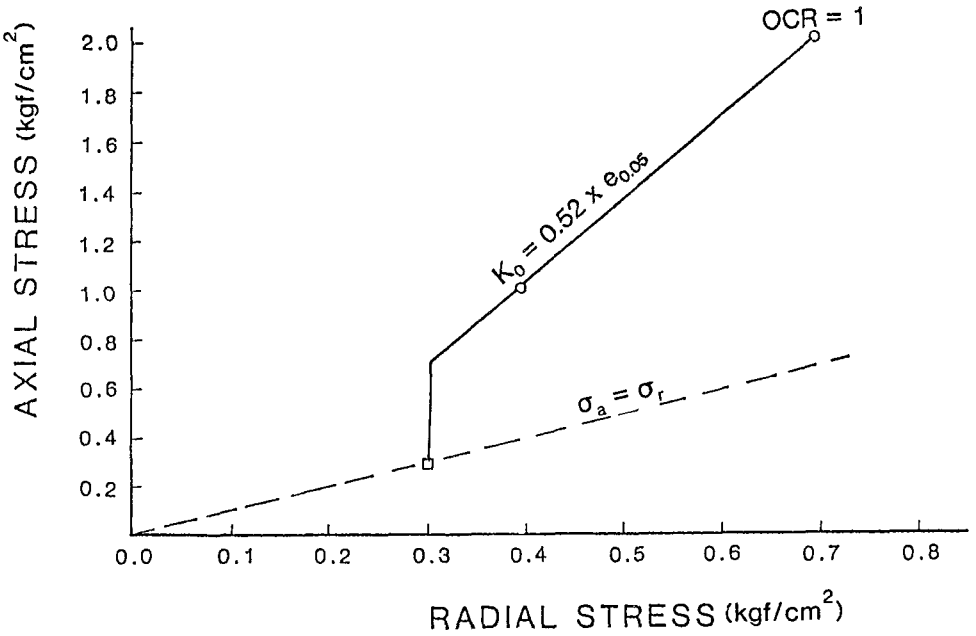

Fig.4 Consolidation paths.

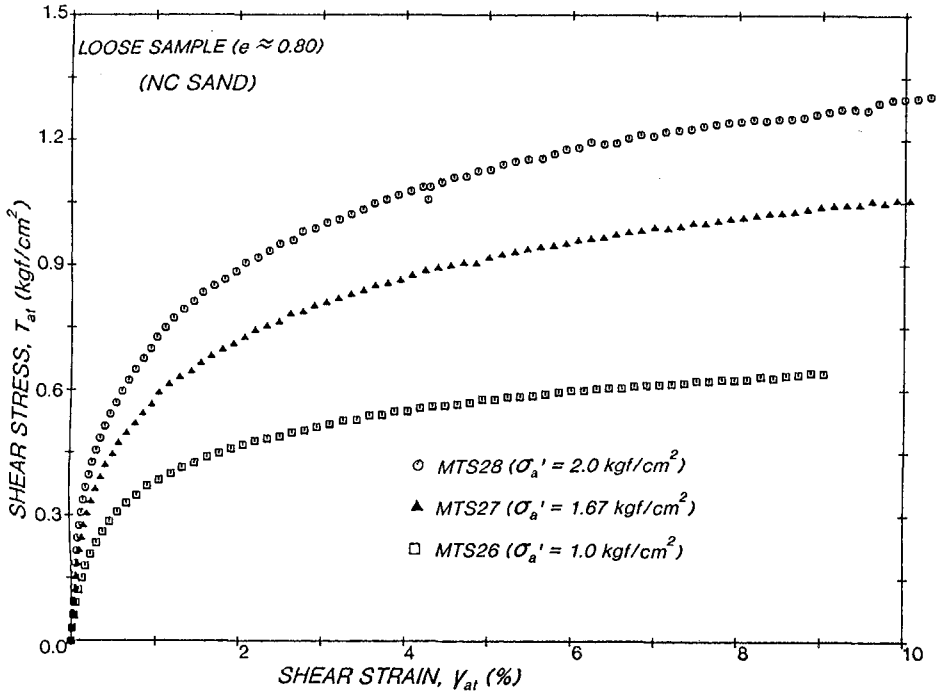

Fig.5 Stress-strain relationship for normally consolidated loose specimens.

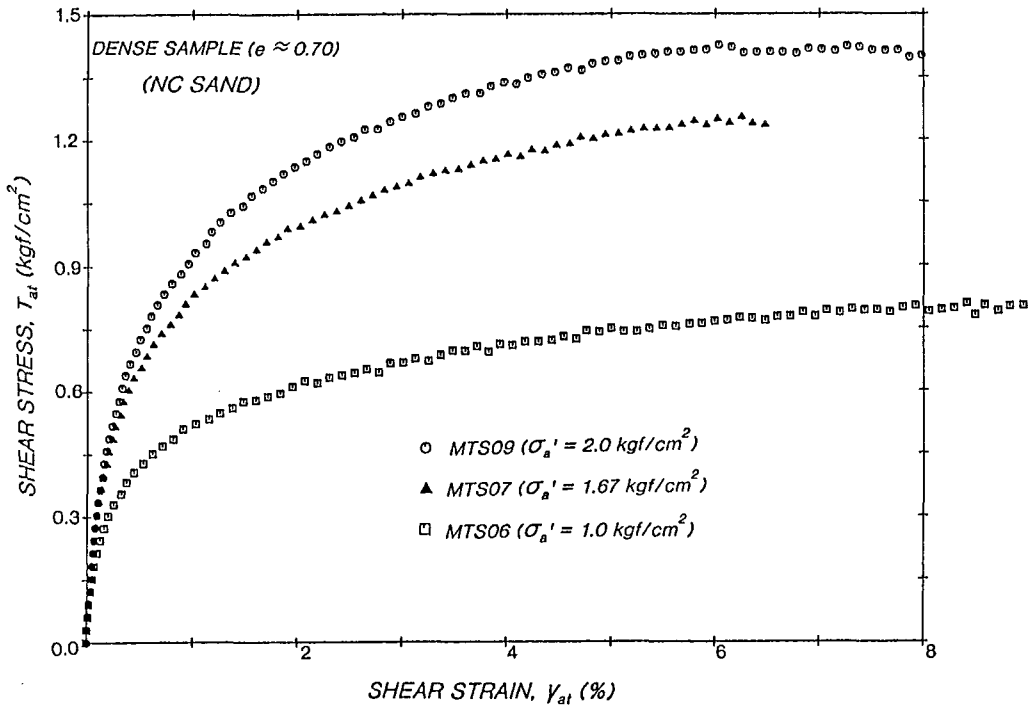

Fig.6 Stress-strain relationship for normally consolidated dense specimens.

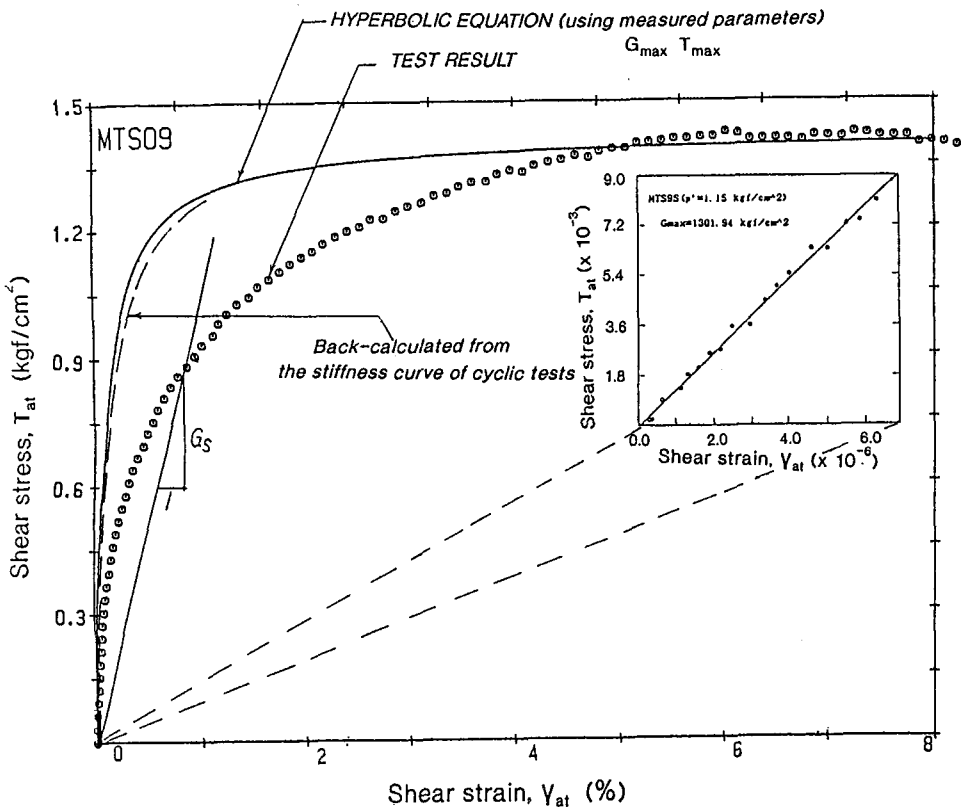

Fig.7 Stress-strain relationship for a dense specimen.

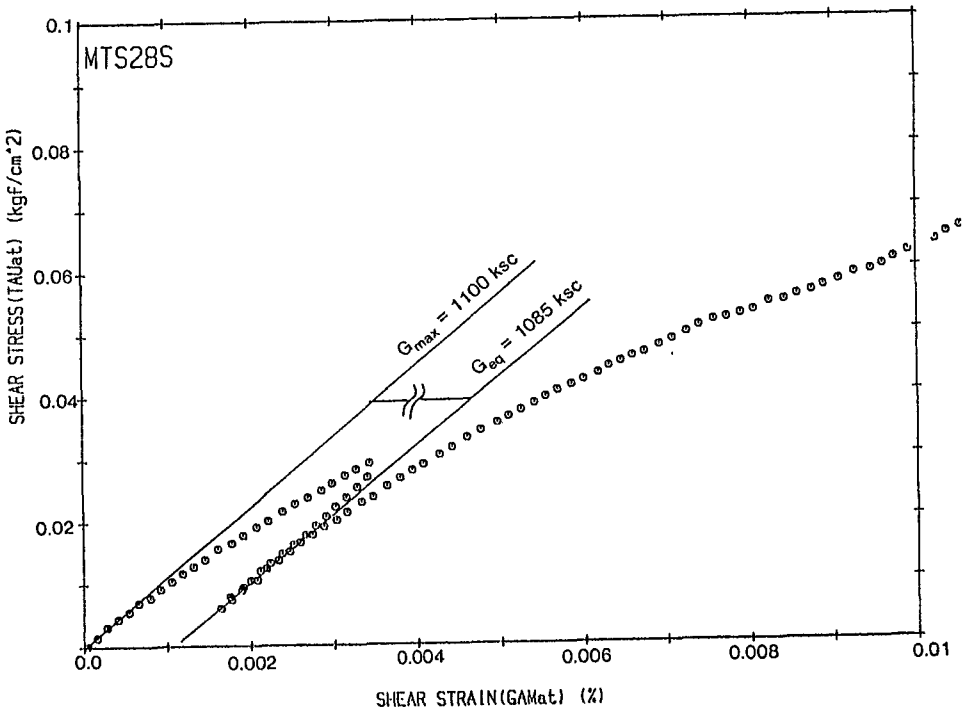

Fig.8 Typical behaviour of an unloading-reloading cycle in a monotonic loading test.

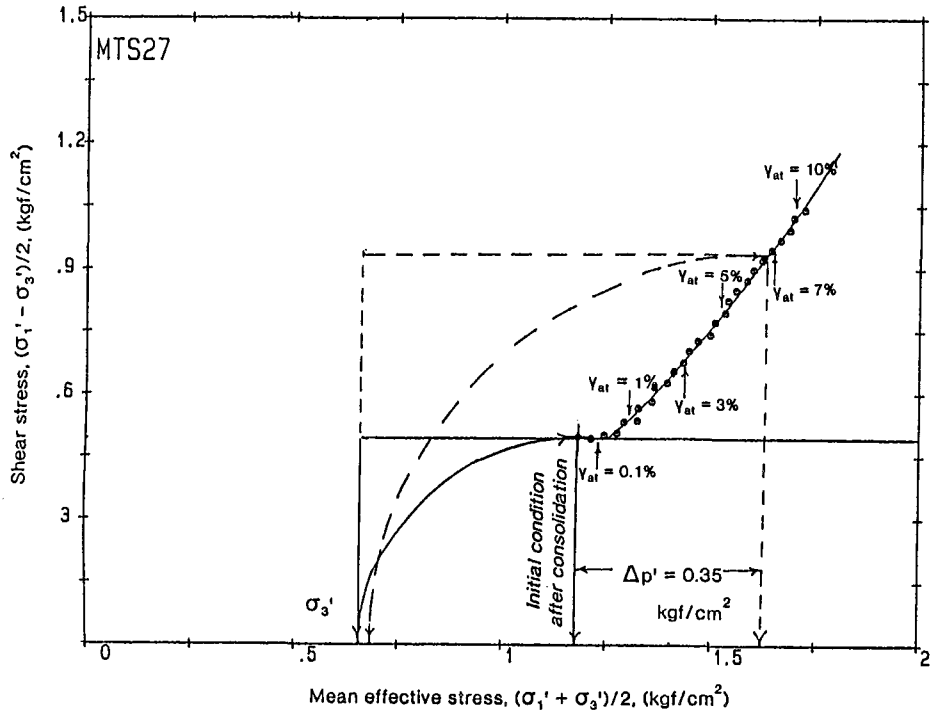

Fig.9 A stress path during simple shear.

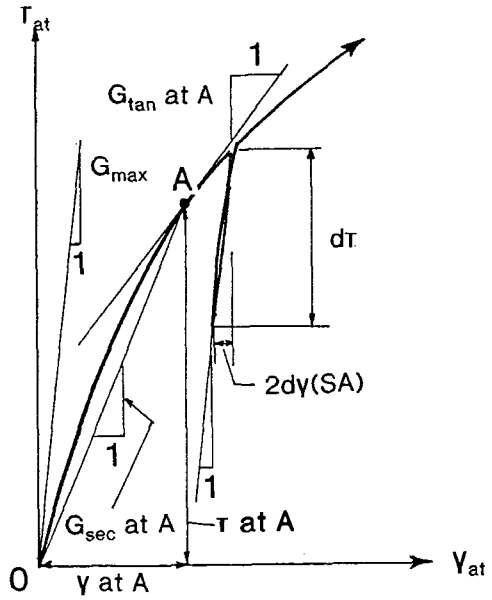

Fig.10 (a)Definitions of shear moduli for the monotonic loading tests.

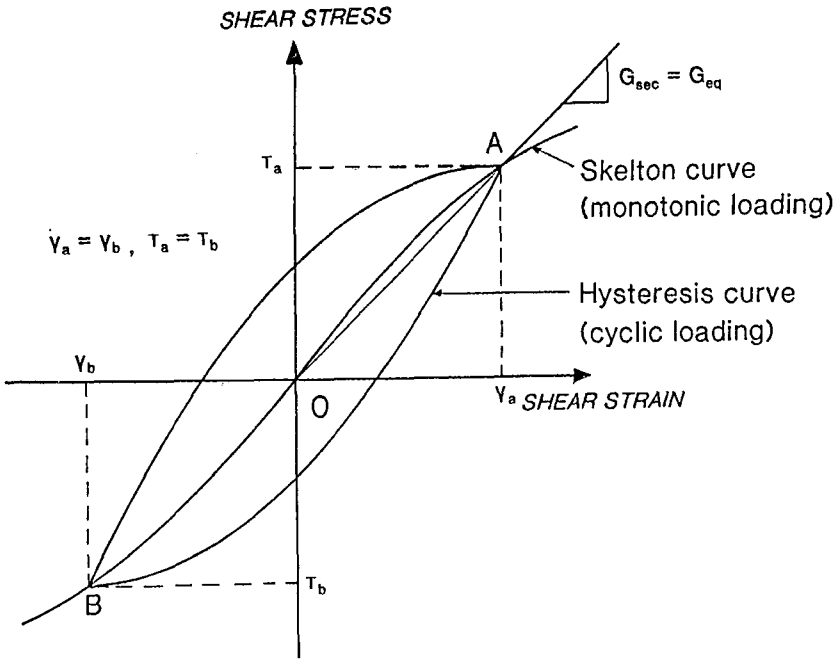

Fig.10 (b)Masing's second rule.

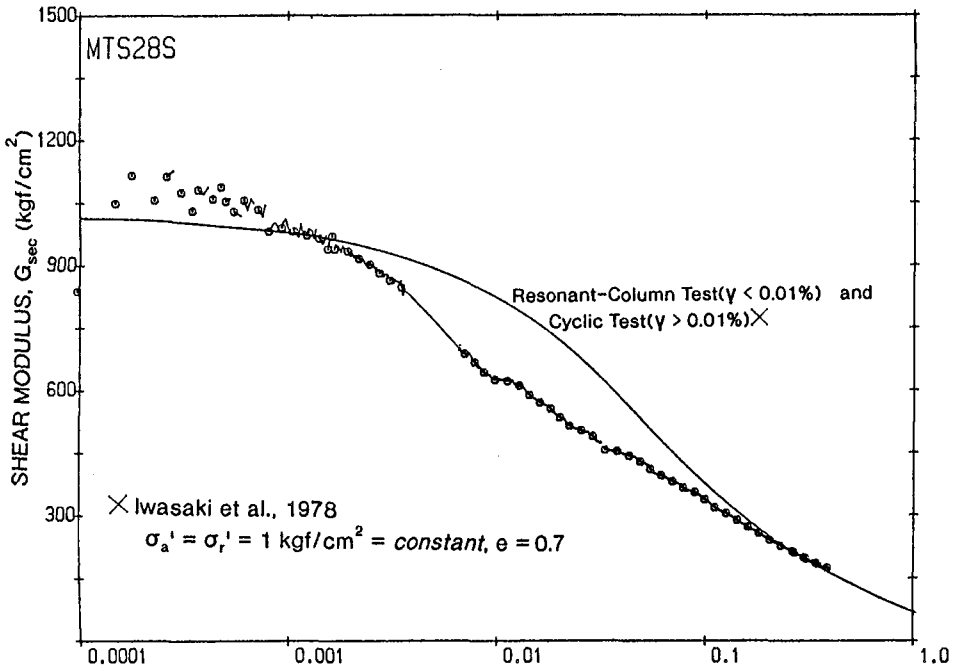

Fig.11 (a) Secant shear modulus versus shear strain for monotonic loading tests compared with those of cyclic tests (dense specimen(Test MTS09))

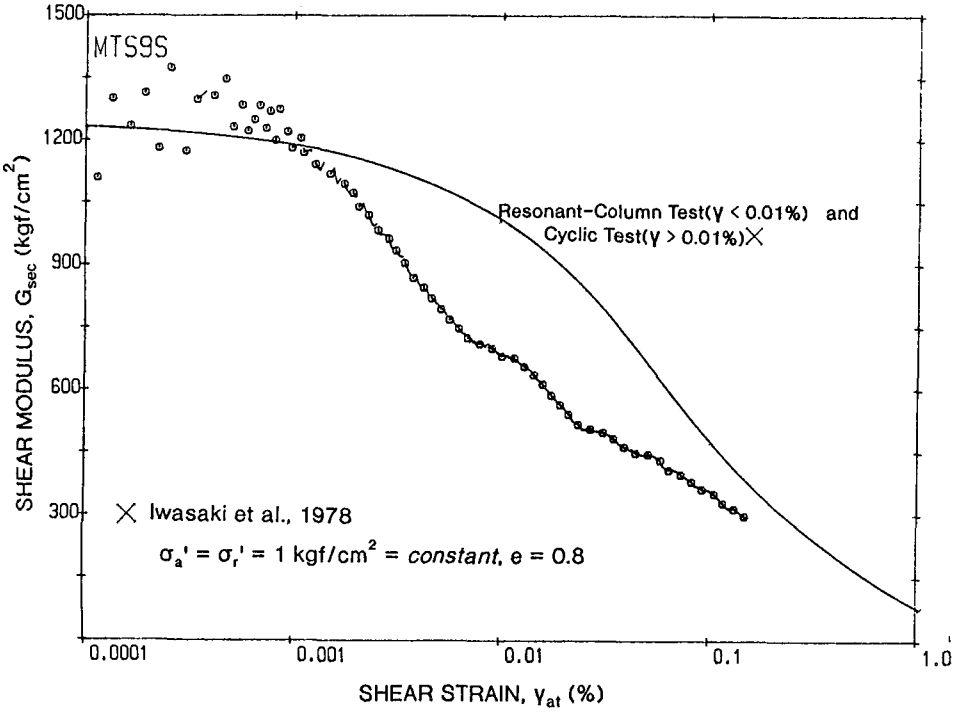

Fig.11 (b) Secant shear modulus versus shear strain for monotonic loadings tests compared with those of cyclic tests (loose specimen(Test MTS28))

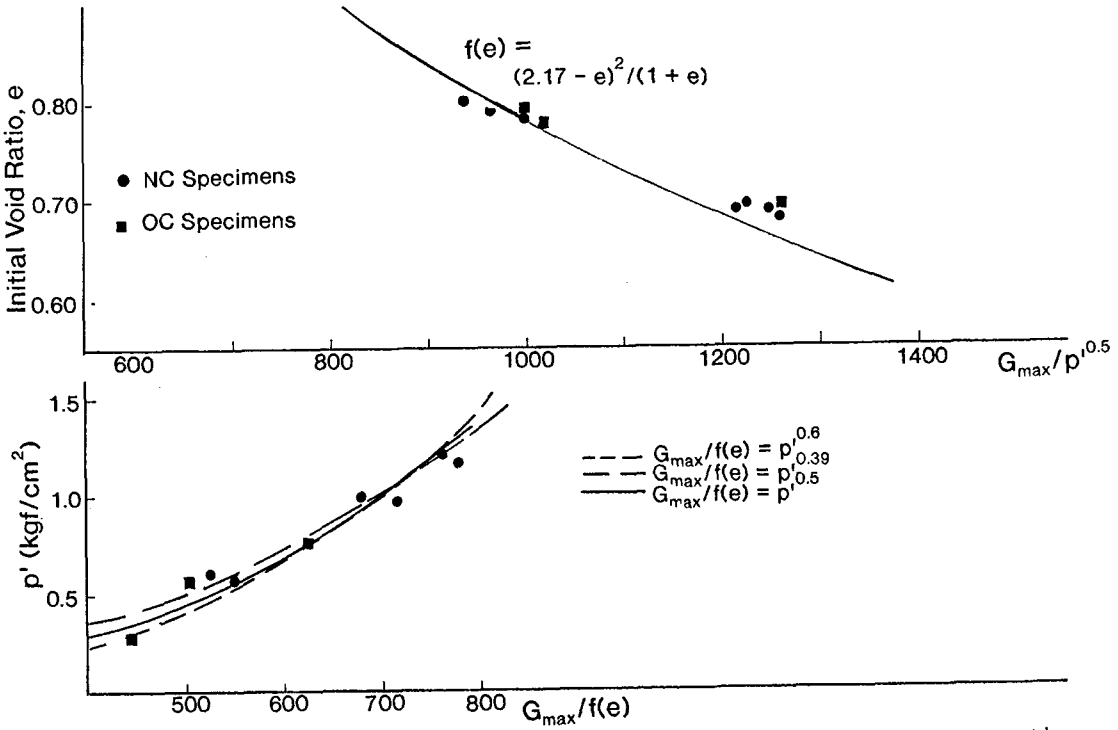

Fig.12 Effects of initial density and mean effective stress on the maximum shear modulus.

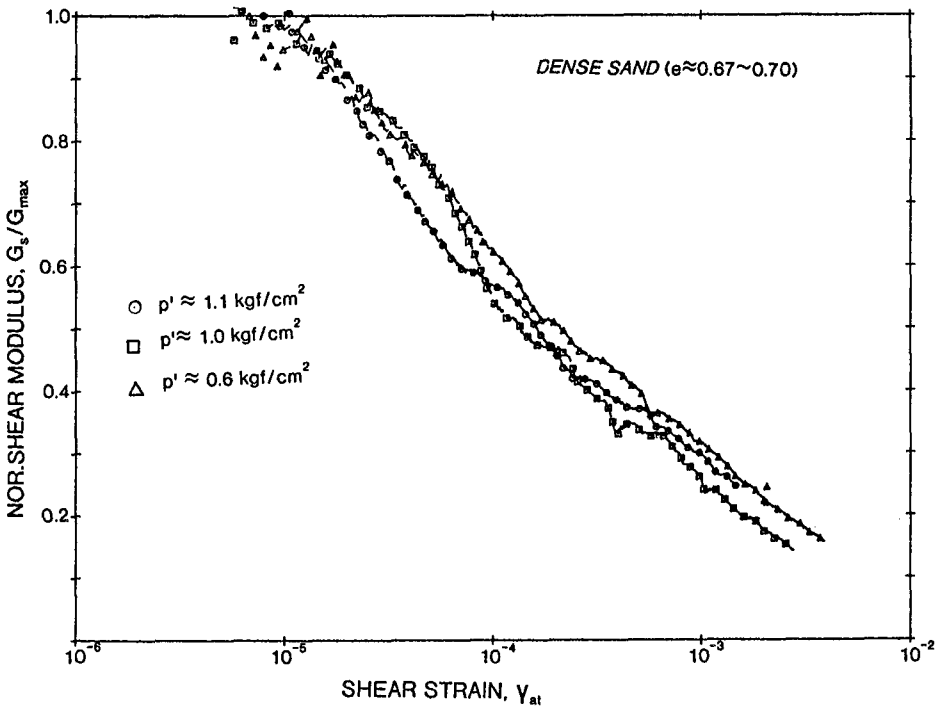

Fig.13 (a) Normalized secant modulus versus shear strain for monotonic loading test(dense specimens)

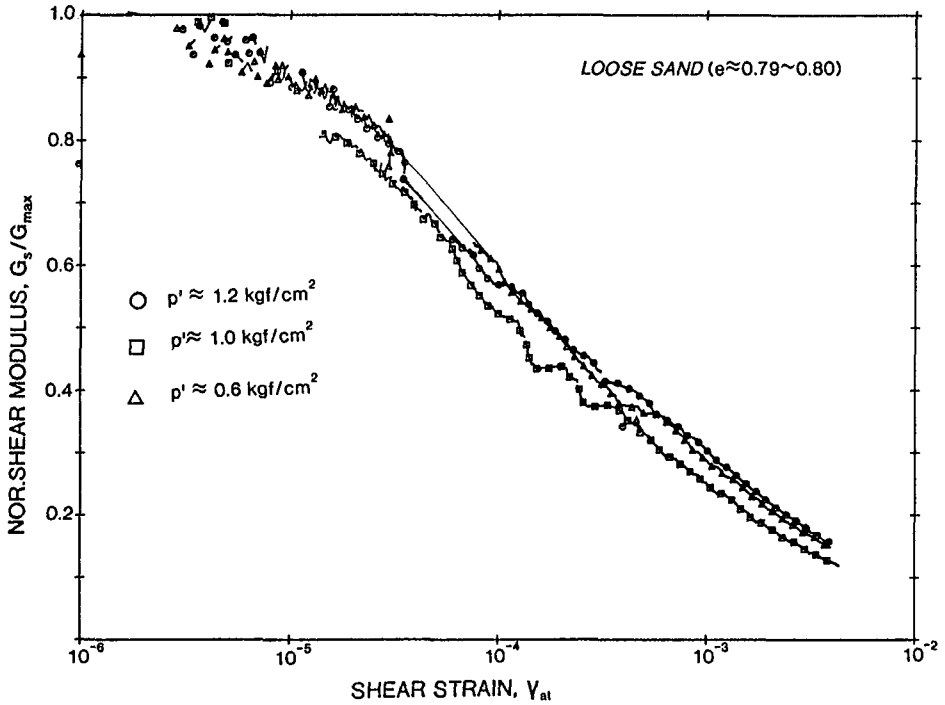

Fig.13 (b) Normalized secant modulus versus shear strain for monotonic loading test(loose specimens)

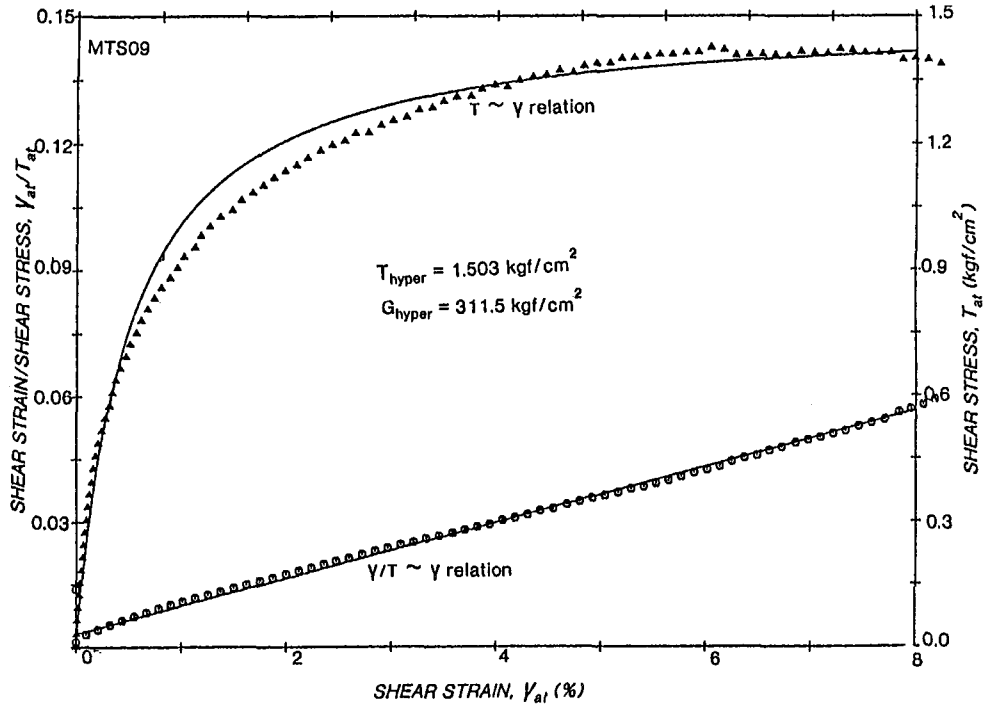

Fig.14 A hyperbolic fitting for the stress-strain relationship.

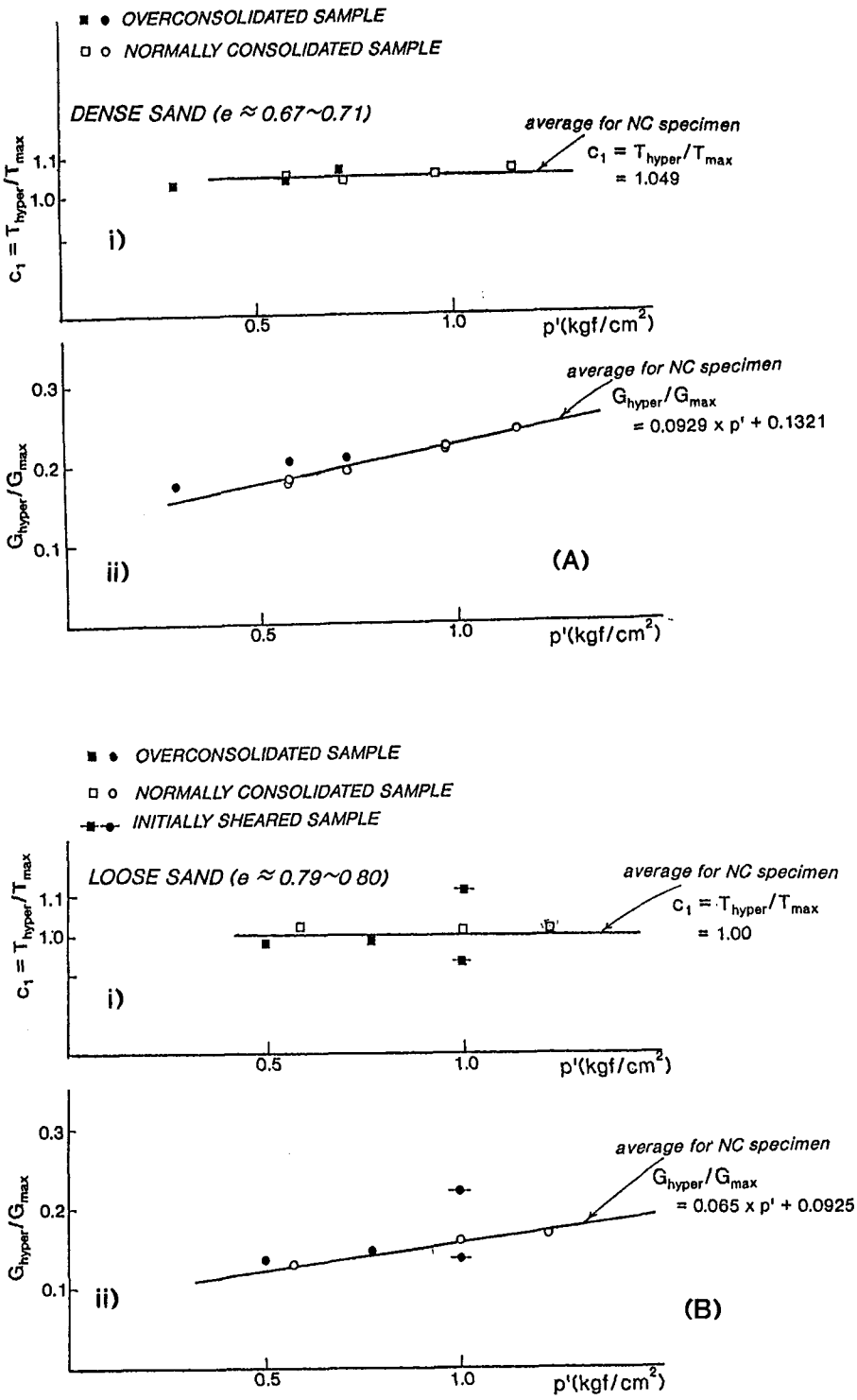

Fig.15 Hyperbolic fitting parameters obtained i) the maximum shear modulus ii) the maximum shear stress (a) dense specimens (b) loose specimens

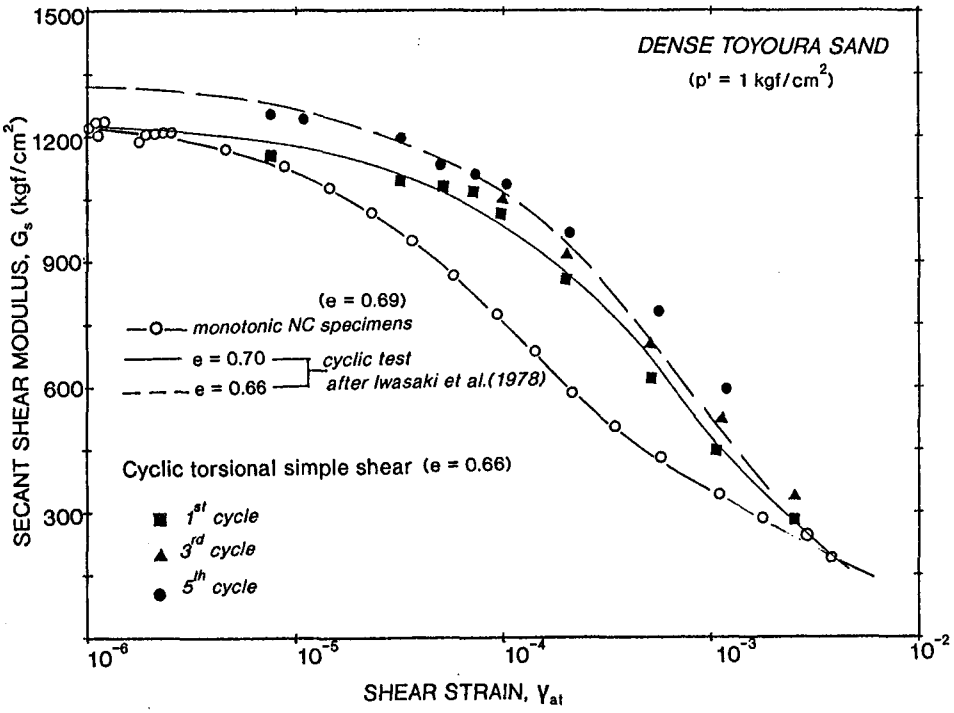

Fig.16 Effects of loading conditions on stiffness

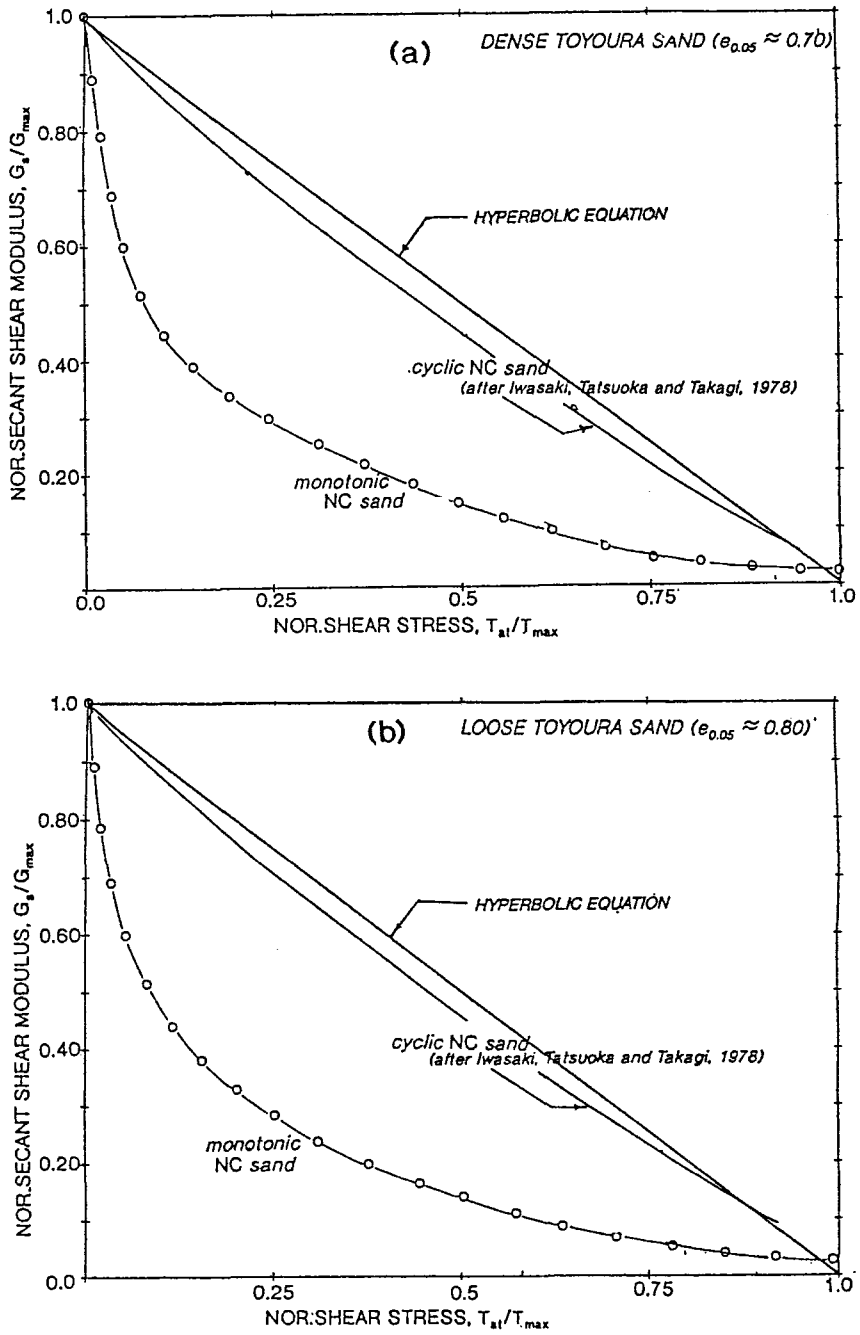

Fig.17 The relationship between normalized shear modulus and the normalized shear stress
(a) dense normally consolidated specimens
(b) loose normally consolidated specimens

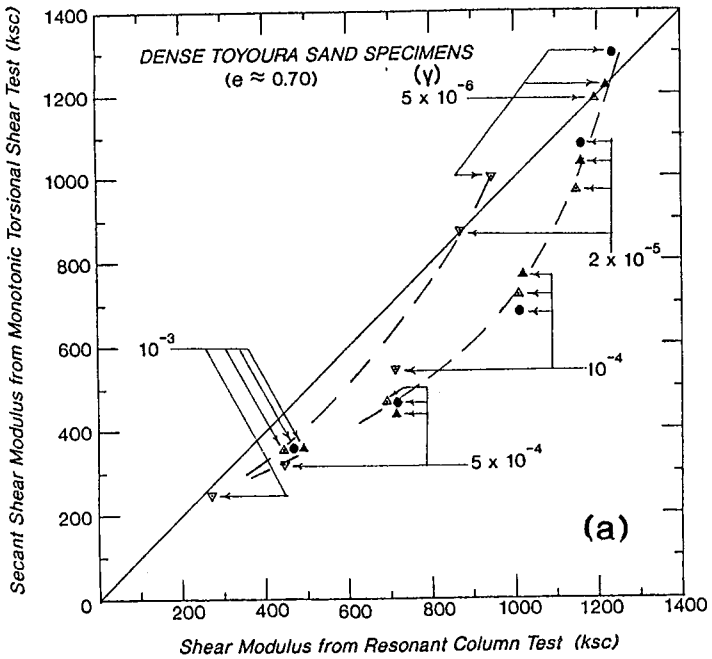

Symbol	p'(ksc)	OCR
●	1.15	1
△ ▲	0.97	1
▽	0.57	1

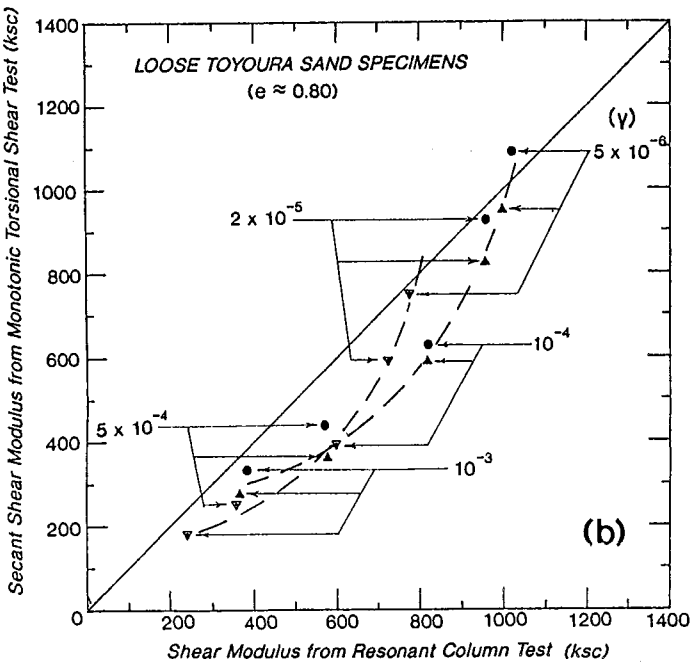

Symbol	p'(ksc)	OCR
●	1.15	1
▲	1.0	1
▽	0.48	1

Fig.18 Comparisons of secant shear moduli between the monotonic loading and the cyclic loading tests.
(a) dense normally consolidated specimens
(b) loose normally consolidated specimens

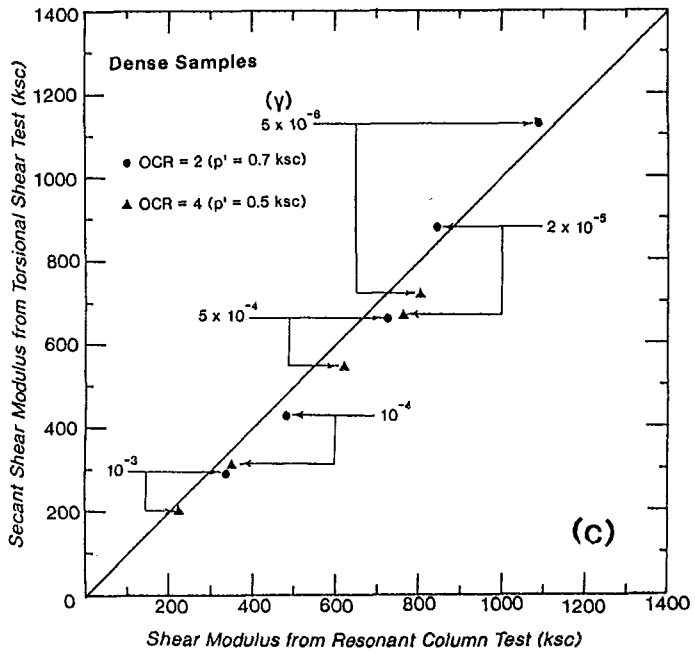

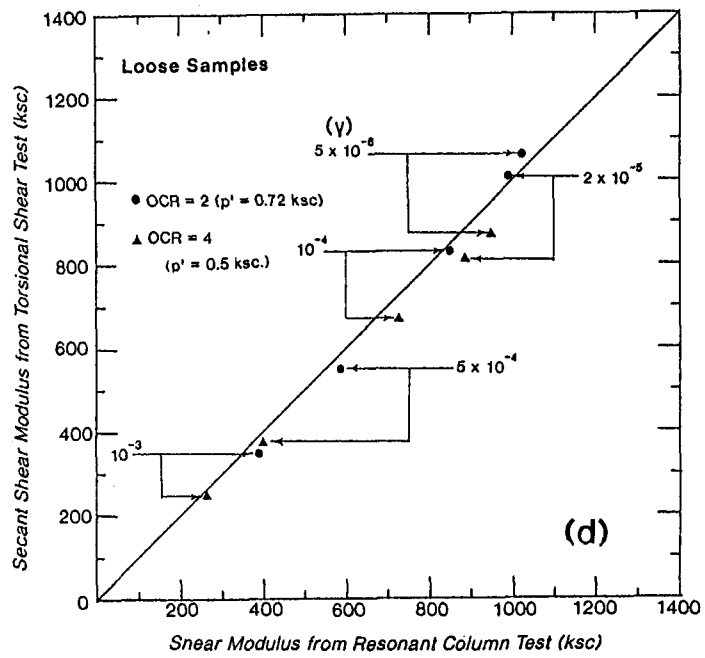

(c) dense overconsolidated specimens
(d) loose overconsolidated specimens